

Preliminary Study on Modeling of the Deformation and Thermal Behavior of FSSW using SPH Approach

Sachin Patil¹, Farzad Baratzadeh^{1,2}, Hamid Lankarani¹

¹ *Mechanical Engineering Department, Wichita State University, Wichita, KS, USA*

² *Advanced Joining and Processing Laboratory, National Institute for Aviation Research, KS, USA*
, Presenting author¹ Tel:+1 (316)2001716, Email: sapatil1@shockers.wichita.edu

Abstract:

Material flow in the solid-state Friction Stir Welding (FSW) is quite a complex process. Investigation of material flow can be carried out either by experimentation or by numerical simulation. However, compared to experimentation, numerical simulation is inexpensive, efficient and convenient, but quite challenging to model. The challenging issue in modeling FSW is to deal with the large deformations of the work piece material. The Lagrangian simulations of FSW show that the severely distorted finite elements are caused due to the large deformation of the workpiece material, which makes the Lagrangian approach inappropriate for modeling FSW. A good alternative is to study it in a SPH environment. SPH formulations are used to overcome the shortcoming of Lagrangian formulations due to its continuous regimes. The basic idea of the SPH approach is that the mesh is obliged to follow material flow. Thereby the excessively distorted elements can be avoided as in Lagrangian formulations. In this paper, we fulfill this aim by using a SPH method. Based on the simulation results, it is concluded that the material motion characteristics on the top surface and through the depth (volume) of friction stir welds have been made for the advancing and retreating sides. The motion trends are consistent with the reported published experimental evidence.

Keywords: *Friction Stir Welding ,SPH Thermal modelling, Kernel approximation, Heat transfer*

1. Introduction

Friction stir welding (FSW) has been studied extensively for the past two decades. There has been a large amount of published work dealing with the FSW analysis, but there has been very little study on the influence of a material flow around tool. This is undoubtedly due to the complexity of the process, which involves mechanical, thermal, and metallurgical phenomena all coupled together. Several authors have considered and proposed to treat the material interactions in FSW, either via numerical simulations but not coupled with the whole trajectory or by developing analytical methods [1-5]. Finite element simulations require discretization of the continuum medium. The equations of a thermo mechanical problem can be written in two different classical formulations: Lagrangian and Eulerian. The Lagrangian representation is the most often used in solid mechanics, where material flow is limited. In the Lagrangian representation, the mesh is attached to material points (also called particles), whereas in the Eulerian representation, the mesh is attached to spatial points. Consequently, during the material flow, in the Lagrangian representation the mesh moves and follows the material points, whereas in the Eulerian representation the mesh is fixed. A mixed representation called the Arbitrary Lagrangian Eulerian (ALE), developed to combine the advantages of the two previous ones, allows the mesh to have a different velocity than the material flow. Adaptive meshing or remeshing is crucial in FSW simulations since the material is so deformed and distorted that the quality of the mesh deteriorate during simulations, leading to numerical problems. To limit the mesh size, the mesh is fine only in a region near the tool. This mesh constraint is attached to the tool. As the tool goes forward, a

remeshing is applied after some time increment which allows one to reduce distortions and to follow the tool [6]. Thermal modeling of FSW is complicated by the coupling of the work done by the FSW tool to deform the welded material and the frictional heat generated [7]. Since direct temperature measurements of the welded zone are not possible, many numerical models have been employed, using the finite element method to account for such complexities such as variable contact resistance [8-10]. Results from these models agree well with experimental data, although they require significant computational resources and set up. Tartakovsky et al.[11] simulated FSW using SPH technique and were successful in studying the effects of process parameters on the temperature field and the associated mixing mechanisms in COMSOL software. This model gave lot of problem regarding contact and no temperature results. It took lot of time in making contact between SPH & language mesh. Other techniques based on Natural element methods (NEM) have also been proposed to model the material flow of the FSW process [12].

In this paper, SPH method is implemented in LS-DYNA in Lagrangian approach whereby the motion of a discrete number of particles is followed in time. A numerical model of the friction stir welding (FSW) process employs discrete smoothed particle hydrodynamics (SPH) to solve the governing equations of conservation of momentum. The advantage of this method over other conventional numerical approaches, such as Lagrangian and Eulerian finite elements and arbitrary Lagrangian Eulerian, is its ability to handle large deformations without failing due to excessive distortion, and be able to explicitly track the material history as in Lagrangian methods. Heat transfer with explicit SPH method can be coupled with structure for thermal stress and thermal structure coupling analysis. New features under development include More thermal BCs for SPH: Boundary _convection, Boundary radiation and so on [13]. This is useful in understanding the plastic deformation and recrystallization process. As part of the attempt to achieve mentioned objectives previously, the Friction stir process evaluated to study material flow and heat evolution.

2. SPH formulation

Smooth Particle Hydrodynamics SPH is a meshless numerical method based on interpolation theory. It allows any function to be expressed in terms of its values at a set of disordered points so-called particles. SPH is not based on the particle physics theory. The conservation laws of continuum dynamics, in the form of partial differential equations, are transformed into integral equations through the use of kernel approximation [14]. SPH is a complementary approach with respect to ALE method. When the ALE mesh is too distorted to handle good results (for example in the case of vortex creation), SPH method may allow to get a sufficiently accurate solution. Smoothed Particle Hydrodynamics (SPH) is a mesh less method for solving physical problems governed by partial differential equations. An important consideration in applying the SPH approach is an advection method which determines the mesh motion in every step of the analysis.

2.1 Numerical method of SPH

The SPH formulation can be divided in two key steps: the integral representation or kernel approximation of field functions and the particle approximation. The concept of integral approximation is to approximate $\int f(x)$ by the particle approximation of a function is:

$$\int f(x) = \int_{\Omega} f(y) W(x-y, h) dy \quad (1)$$

with h the so-called smoothing length and W a kernel approximation such that:

$$\forall x, \int_{\Omega} W(x-y, h) dy = 1 \quad (2)$$

$$\text{and } \forall x, \lim_{h \rightarrow 0} W(x - y, h) = \delta(x - y) \quad (3)$$

where δ denotes the Dirac function. A kernel based spline function developed by Monaghan and Lattanzio (1985) will be used in most simulation:

$$W_{ij} = \begin{cases} \frac{1}{\pi h^3} \left(1 - \frac{3}{2}q^2 + \frac{3}{4}q^3 \right) & \text{if } 0 \leq \frac{x}{h} \leq 1 \\ \frac{1}{\pi h^3} \left(\frac{1}{4}(2-q)^3 \right) & \text{if } 1 \leq \frac{x}{h} \leq 2 \\ 0 & \text{otherwise} \end{cases} \quad (4)$$

where $q = x/h$; x = distance between particles i and j and h = smoothing length in SPH. This smoothing length, which is often called as the influence domain or smoothing domain, controls the size of the area around particle i . It is better to have a variable smoothing length to avoid problems related with expansion and compression of material. The concept of a variable smoothing length was developed by W. Benz[14] to keep enough particles in the neighborhood to validate the approximation of continuum variables. The smoothing is allowed to vary in time and space. A scheme of this kernel based search is shown in Fig 1.

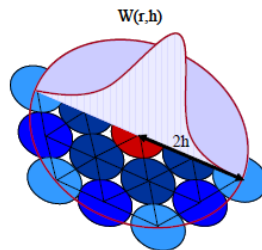


Fig 1: Kernel based on spline functions [14]

In the SPH analysis, the interpolation depends on interactions of particle with its neighbors. Therefore, a neighboring search technique has been developed Lacombe [15]. For the neighboring search, the bucket sort algorithm is used. The domain covered by the particles is split in several boxes of a given size. First the algorithm searches for neighbors, for each particle inside the main box and the neighbor boxes contained in the domain of influence of the particle. Both fundamental equations Continuity and Momentum normalize by weighting with an approximation i.e. Kernel function W_{ij} . In an explicit transient dynamic simulation, the momentum equation is solved using a central difference time integrator as efficient SPH computation process.

$$\rho \frac{\partial(v)}{\partial t} + \nabla \cdot \sigma = 0 \quad (5)$$

In above equation, ρ is the material density, v is the material velocity, and σ is the Cauchy stress. Using the above gradient methods for evaluating the strain rate from the velocity field, and using appropriate constitutive equations, stress increments can be calculated. Finally, the divergence of the stress field is evaluated, and each node was occupying a volume V with mass ρV is accelerated accordingly. In this manner the motion of the nodes is driven by the mechanics being simulated. Relevant field quantities are re-evaluated at each time step and at each 1/2 time step as required by the central difference time integrator. Equations of state to represent the material behavior, is being investigated as a viable alternative [16].

$$P = B \left[\left(\frac{\rho}{\rho_0} \right)^\gamma - 1 \right] \quad (6)$$

where $\gamma = 7$ and $B = c_0^2 \rho_0 / \gamma$, $\rho_0 = 1,000 \text{ kgm}^{-3}$ which is equal to the reference density and $c_0 = 16.3 \text{ m/s}$ the speed of sound at the reference density .

2.2 SPH FSSW Model setup

An initial attempt to develop a fully coupled thermo-mechanical model for the plunge phase of the modified refill FSSW done here. Similar to the Friction Stir Welding, the Spot Welding process also consisted of light materials as aluminum except tool doesn't follow a linear motion alongside the work piece. Fig 2 shows a Schematic description of the FSSW model. During the FSSW process, a rotating pin tool plunges into the upper sheet of a lap joint. Heat generated by the rotating pin softens the surrounding material and facilitate further penetration of the tool. Severe plastic deformation of the surrounding material forms a bond along the periphery of the pin. Finally, the rotating pin tool is retracted, leaving the characteristic keyhole in the center. The goal was to obtain a model with a calculation time as short as possible and which can predict material flow. Several assumptions were made to reduce the model size and the computation time, allowing the development of a useful method.

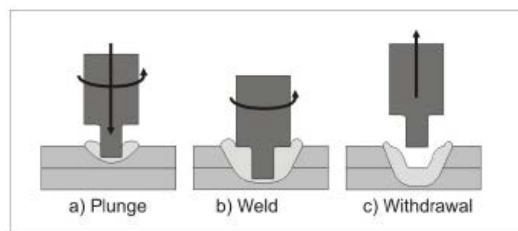


Fig 2: Schematic of the FSSW process

2.2.1 Material formulation

The aluminum 6061-T6 work-piece material is modeled as elastic, hardening-plastic. Typical Mechanical Properties are Ultimate Tensile Strength 45 ksi , Yield 40 ksi and Elongation (17 %). Like the FE method, the SPH method will admit any reasonable material constitutive model. In these analyses the material model *015 MAT_JOHNSON_COOK visco plastic constitutive model J2 plasticity used. In LS-Dyna keyword manual [16], this is referred as the elastic plastic with kinematic hardening material model with strain-rate effects.

The Johnson Cook expresses the flow stress as:

$$\sigma = \left[A + B \bar{\epsilon}^n \right] \left[1 + C \ln \dot{\epsilon} \right] \left[T^* \right]^m \quad (7)$$

Here, is σ the effective Cauchy stress, $\bar{\epsilon}$ is the equivalent plastic strain (a dimensionless quantity), $\dot{\epsilon}$ is the equivalent plastic strain rate (effective strain rate divided by $\dot{\epsilon}_0 \text{ s}^{-1}$, so that it is also dimensionless), $\frac{\dot{\epsilon}}{\dot{\epsilon}_0}$ is the normalized equivalent plastic strain rate (typically normalized to a strain rate of 1.0 s^{-1} and T^* is the homologous temperature, which is another dimensionless quantity defined by

$$T^* = \frac{T - T_0}{T_M - T_0}, \quad (8)$$

Where $T_0 = 20\text{C}$ is room temperature, and T_M is the melt temperature of the material. Here stress-strain curves are modeled using coefficients A, B and n, as defined in equation (7). The strain rate dependence was included through the coefficient C in the model

The Johnson-Cook material model requires an equation of state for determining hydrostatic stresses. At high pressures, attempts have been made to make the yield dependent on pressure. An equation of state [17,18] can be considered a constitutive law for relating pressure P or hydrostatic stresses and hydrostatic strains or specific volume V. An Equation of State. *EOS_LINEAR_POLYNOMIAL was used, setting C1 to the bulk modulus and all the other C terms to zero. The parameters for material AL 6061- T6 used in these analyses are adapted from [19,20]: A= 325 Mpa, B=411 Mpa, n=0.373, C=0.014, m=1.58.

The cutting tool is rigid (no deformation) steel and the material model *MAT _020_RIGID was used. In these analyses a consistent set of units were used; namely, cm, g, μ s to reduce the numerical error in each time step.

The model of the 3D work-piece and FSSW tool is shown in Fig 3(a). Dimensions of the work-piece are kept small, being about 30mm x 20 mm x 4mm in this preliminary model. This model is a rectangular sheet. The model was meshed using SPH elements, a total of 280000 elements used. Tool Geometry is shown in Fig 3(b). It is a threaded tool with chamfer bottom instead of the Flat bottom. Threads of the friction stir welding tool pin were left hand screw threaded such that the tool rotation will be anticlockwise. The Tool in the analysis modeled with solid tetrahedral elements is a threaded tool of diameter 6 mm, Shoulder diameter 14 mm and height of tool 4 mm. The tool has given Angular velocity 1000 rpm and Plunge velocity 2 mm/sec. The plunge velocity can be increased 10 times higher than the real velocity to reduce computation time from 20 hours to 1 hour 50 min. However, the final calculation should always be carried out without process time scaling. In this real simulation velocity used since the work piece material model is of the rate dependent type, the change in velocities will have a significant effect on the simulation results [20]

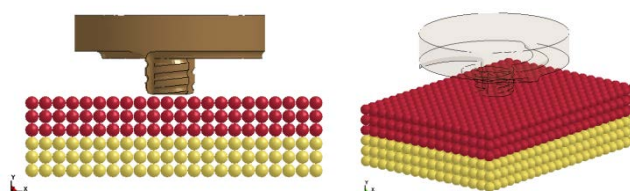


Fig 3: (a) SPH model geometry of FSSW

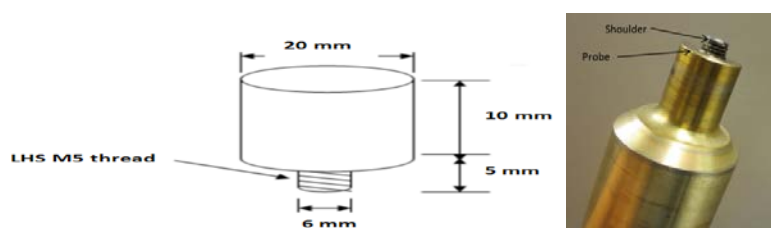


Fig 3 : (b) Tool geometry for FSSW

The pin and shoulder, rigidly constrained together, are modeled as rigid cylinders since they are made of a material of heat treated steel much stiffer than the work piece material of aluminum alloy 6061-T6. The interface between the work pieces and tool is frictional contact with a frictional coefficient of 0.5. The SPH method predicts the force output proportional to the friction coefficient studied. Heat transfer with SPH method applied here from the paper of J. Xu [21]. An explicit formalism for heat conduction with Smoothed Particle Hydrodynamics method was developed in LS-DYNA code. A series of simple test problems were used to demonstrate the capabilities of LS-DYNA in thermal option with SPH particles. The thermal boundary condition for SPH particles imparted through keyword *BOUNDARY_TEMPERATURE_OPTION and BONDARY_FLUX_ boundary condition applied to the surface segments of SPH particles. Also, Thermal material property identification (TMID in *PART card) defined in the *MAT_THERMAL keyword has to be specified for the thermal option of SPH. Initial temperature condition can be applied to the SPH particles through keyword: *INITIAL TEMPERATURE OPTION, Thermal boundary condition for SPH particles can be realized through keyword: *BOUNDARY TEMPERATURE OPTION. These two thermal conditions will be applied to the SPH particles directly. The thermal option for SPH can be activated by setting SOLN-2 in *CONTROL SOLUTION card. The parameter Eq heat (mechanical equivalent of heat conversion factor) and fwork (fraction of mechanical work converted into heat) in *CONTROL_THERMAL SOLVER card can be used for coupling thermal structure analysis

2.2.2 Contact Definitions

The contact along the interfaces between the work piece and welding tool (i.e. pin and shoulder) is assumed as frictional contact with a frictional coefficient of 0.47[22]. In order to model the transfer load between the tool and the target work, it was used a CONTACT-AUTOMATIC-NODES-TO-SURFACE Card (Fig 4), for which each slave node is checked for penetration through a master segment. In tied contact types, the slave nodes are constrained to move with the master surface, i.e. the tied contact surfaces "glue" the slaves to the masters. The slave and master segments should initially be coplanar. This is a constraint-based contact in which the forces are computed to keep the slave nodes on the master surface

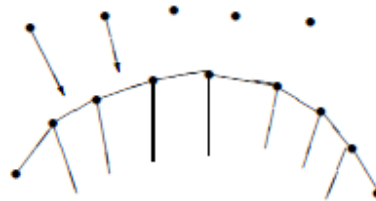


Fig 4: Contact automatic nodes to surface and Contact tied surface to surface [22]

2.2.3 Accuracy of the FE analysis

In explicit analysis, if the time step size of an element is small, the cost of the analysis will be more. To overcome this, nonphysical mass is added to the elements to achieve larger time step which will, in turn, reduce the cost of the analysis. The structural time step can be increased by scaling the density of the elements by a scale factor. In a coupled thermal analysis, in addition to the structural time step, the thermal time step should also be increased to achieve the numerical stability.

This can be achieved by scaling the specific heat capacity by a scale factor. The increase in the mass of the elements in a dynamic analysis also increases the acceleration and will result in over prediction of forces. If the kinetic energy is very small relative to the peak internal energy, then the addition of mass will not affect the results.

Two simulations were run with one having no mass scaling and another with a mass scaling factor of 100. Fig 5 shows the ratio of the kinetic energy to the peak internal energy for both simulations. The KE/IE ratio was only 0.1% for the analysis with no mass scaling and 25% for the analysis with mass scaling. The ratio should be less than 10% for an acceptable solution [16]. Thus mass scaling won't lead to an accurate solution.

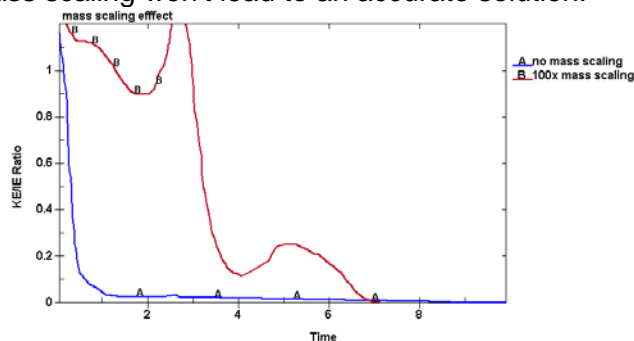


Fig 5: KE/IE ratio of the analysis

2.2.4 Temperature & flow pattern study

Heat generation dominated by tool rotation. Two SPH particles located around tool 2.5 mm from center seen in Fig 6 and 7 below. Both particles has same temperature at beginning. P2 is displaced lesser than P1 thus showing less temperature. Average temperature observed is comparable to Experimental data obtained from Gerlich et al. [23], in which temperature measured at the tool tip during plunge into Al 6111.

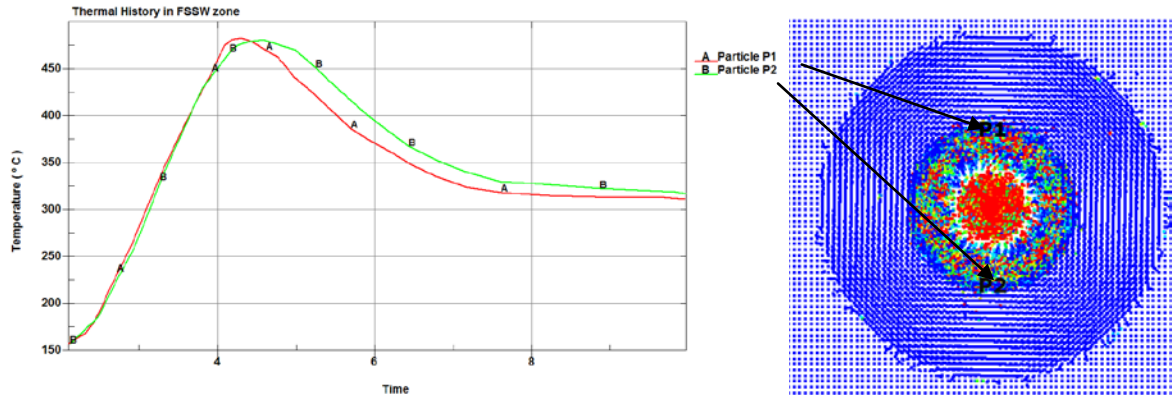


Fig 6: Temperature history for particle P1 and P2

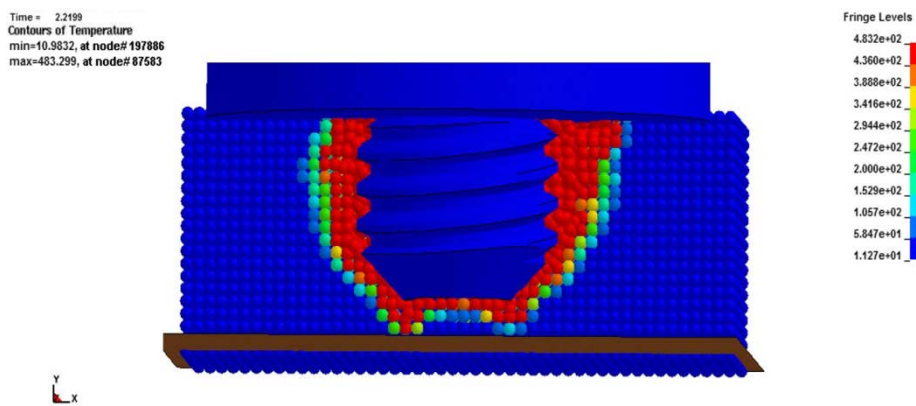


Fig 7: Temperature Contour

Flow pattern can be studied by observing the movement of nodes from Bottom views of a work piece and tool, at the start and end of the simulation shown in Fig 8. The SPH particles show a combination rotational and downward motion due to plunging.

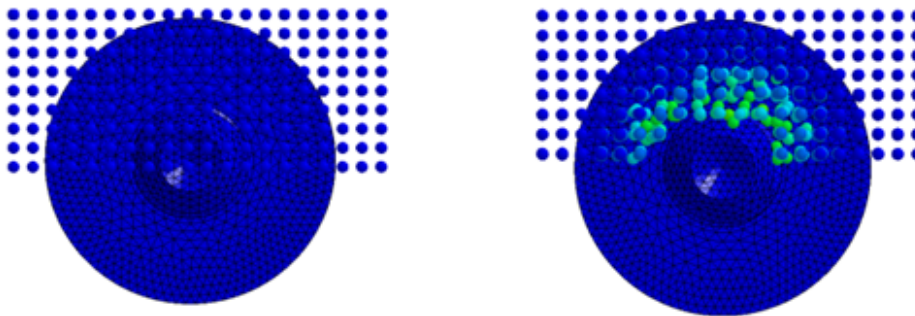


Fig 8: Bottom views of a work piece and FSW tool, at the start and end of the simulation

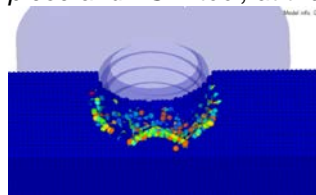


Fig 9: Material flow around pin

Tool wall was moving SPH Elements as trajectories as seen in Fig 9. Elements initially located in the path of the tool, separated by nearly equal distances. For better visualization of

material flow would need a much higher resolution for SPH spacing, However, this would highly increase the computational cost. SPH node spacing of 0.1 mm (fine) and 0.05mm (very fine) tried for this analysis. Convergence of the SPH calculation is investigated by examination of the convergence of reaction force on the tool.

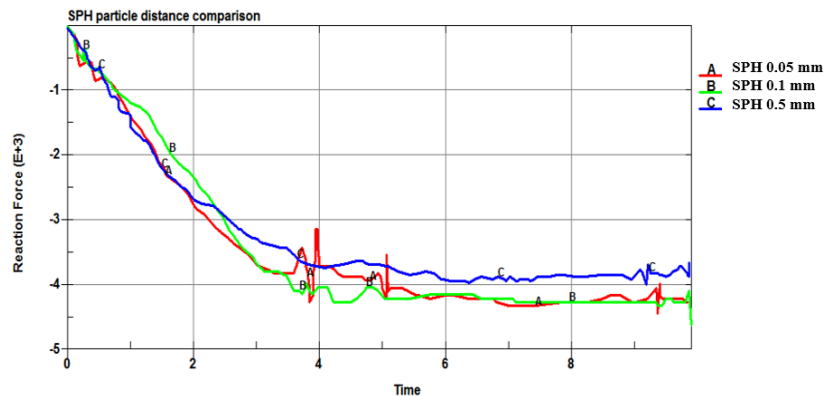


Fig 10: Comparison of different SPH Mesh particle distances in weld zone

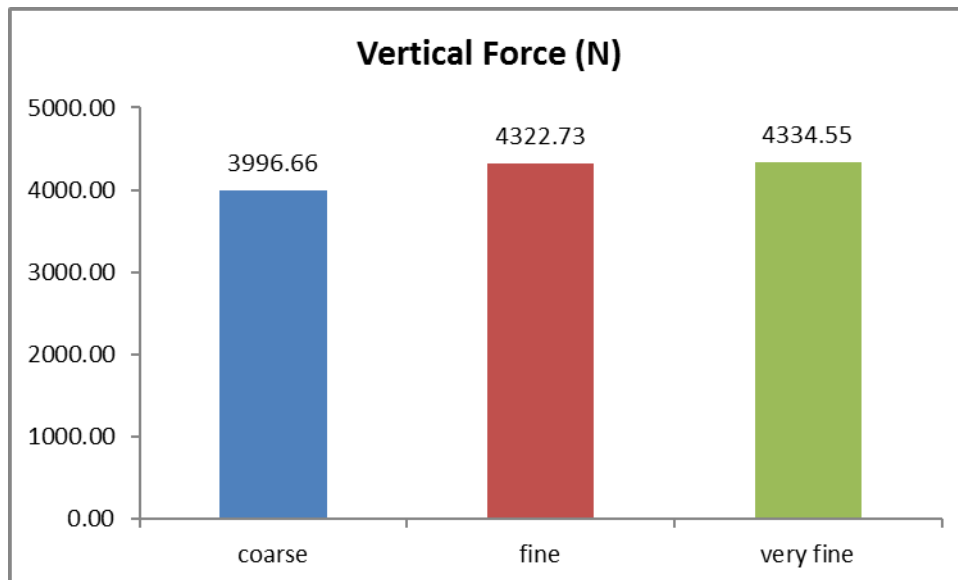


Fig 11: SPH mesh sensitivity Analysis

Fig 10 compare of different SPH Mesh particle distances in the weld zone. The SPH behavior for reaction force response is closer for Particle distance 0.1 mm and 0.05 mm, compared to original 0.5 mm. SPH node spacing of 0.1 mm (fine) and 0.05mm (very fine) tried for this analysis. Fig 10 shows vertical force 4.3 KN on the tool. The forces calculated from SPH simulation match approximately to 5.5 KN experimental data (Fig 11) obtained from literature Gerlich et al. [23], although used the comparable material for study.

2.2.5 Other Numerical results (Fig: 12-15)

Plots of Von-Mises stress contour near tool shown in Fig 12 corresponds to material yield stress and The stress fields are in good agreement with observations in the literature [17].As it can be observed in following d3plots(Fig 13), the plastic strain reaches the value of 2.38 to 4 maximum and is generated close to the tool periphery, since the material is subjected to intense deformations due to the rotational motion. This issue matches with the maximum temperature found in the same zone.

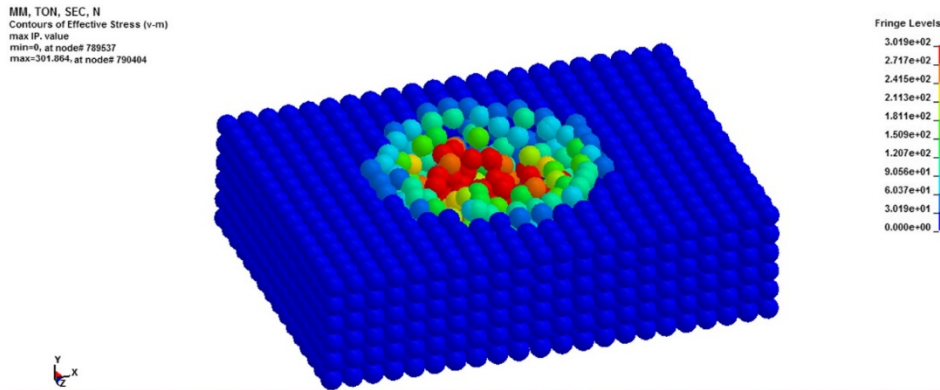


Fig 12: Plots of Von-Mises stress contour near tool

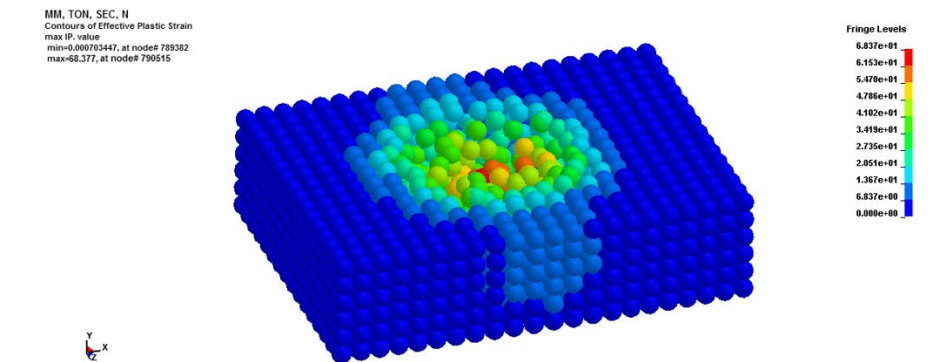


Fig 13: The effective plastic strain field around the tool.

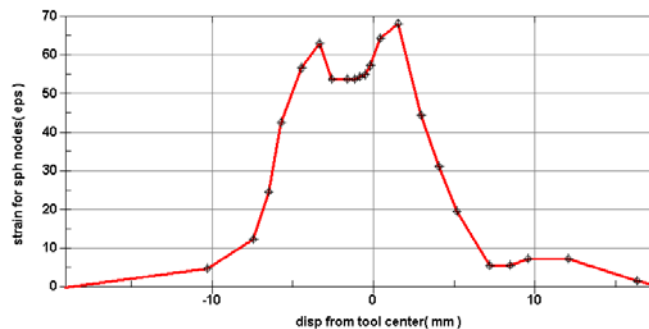


Fig 14: Strain variation for SPH nodes in weld zone

From the observed d3plots plastic strain contour, strain distribution pattern can be plotted as shown in above Fig 14. Few nodes are selected in weld zone to track down plastic strain values. In this model, strain reaches the value of 68 maximum, and corresponding strain rate found 8 1/s. Strain and strain rate found lower due to the scaling of velocity to reach numerical stability. However reported strain rate values varied from 4 to 3000 in various literature [5,20]. Also, maximum strain occurs on advancing as expected due to more friction of the shoulder on this side. To conclude, an image of the 3D simulation of a stir zone is presented in Fig 15 which demonstrates some degree of conformity of the simulated material flow with experimental observations [24]

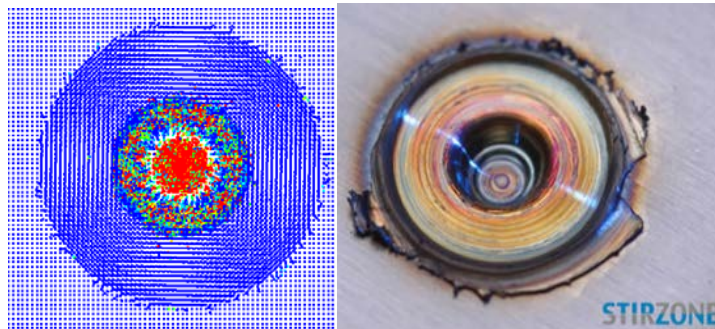


Fig 15: Stir Zone qualitative comparison

Conclusion

SPH method in LS-Dyna can capture the main processes involved in the stir zone. Shekhar et al [25] shown material flow in their work without thermal effect. The SPH code, as implemented in LS-Dyna, is an updated one, which allows now to implement thermal conduction in SPH. However, it is difficult to describe the contact between the work and tool edge. Although the above analysis made for Al6061-T6 material, present model also able to work properly for other material to develop further. SPH method predicts frictional behavior rather well and considerably better than the Finite Element Method. However, further studies have to be carried out to determine a friction coefficient. The lack of consistency of SPH in regions where the kernel loses some of its support (i.e. near surfaces). Some modification required to the standard SPH method to remedy this deficiency. Comparison to the experimental results showed that the SPH model in LS-Dyna performs very well as long as the tool sink /plunge down. For longitudinal movement of tool, material doesn't flow laminar. This complex flow could not readily be explained, nor was detailed information found in the literature, where the same evolution has been encountered. A test case is suggested for further study. A mesh sensitivity study was performed with respect to mesh density in order to ensure that the SPH mesh was fine enough to give reliable results.

REFERENCES

- [1] Chao, Yuh J.; Qi, Xinhai, 1998, "Thermal and Thermo-mechanical Modeling of Friction Stir Welding of Aluminum Alloy 6061-T6", Journal of Materials Processing & Manufacturing Science, p 215-233.
- [2] Song, Mingde; Kovacevic, Radovan; Ouyang, Jiahu; Valant, Mike, 2002, "A Detailed Three-Dimensional Transient Heat Transfer Model for Friction Stir Welding", 6th International Trends in Welding Research Conference, p 212-217.
- [3] Khandkar, Mir Zahedul H.; Khan, Jamil A.; Reynolds, Anthony P., 2002, "Input Torque Based Thermal Model of Friction Stir Welding of Al-6061", Trends in welding research : proceedings of the 6th International Conference, Callaway Gardens Resort, Phoenix, Arizona, p 218-223.
- [4] Chao, Y. J. and Qi, W., 2003, "Heat Transfer in Friction Stir Welding-Experimental and Numerical Studies," ASME Journal of Manufacturing Science and Engineering, 125, pp. 138-145.
- [5] Goldak J., Chakravarti A., and Bibby M., "A New Finite Element Model for Welding Heat Sources, Metallurgical Transactions," 158(2), 299-305, 1983.
- [6] A.A. van der Stelt, H.J.M. Geijselaers, W. Quak, R. Akkerman, J. Huetink, "Comparison of ALE finite element method and adaptive smoothed finite element method for the numerical simulation of friction stir welding" AIP Conference Proceedings, Volume 1353, Issue 1, 10.1063/1.3589694

- [7] Nandan, R., DebRoy, T., and Bhadeshia H. K. D. H., "Recent Advances in Friction Stir Welding Process, Weldment Structure and Properties," Pennsylvania State University, University Park, PA, 2008.
- [8] De Oliveira, P.H.F., Amancio Filho, S.T, dos Santos, J. F., and Hage, E. Jr., "Feasibility Study of the Friction Spot Welding (FSpW) Process in Thermoplastics—Estudo de viabilidade da soldagem de termoplásticos por 'Friction Spot Welding' (FSpW)," *Soldagem & Inspecao*, 17(2), 96–103, 2012.
- [9] Colegrove, P.; M. Painter; D. Graham, and T. Miller, 2000, "3 Dimensional Flow and Thermal Modeling of Friction Stir Welding Process, 2nd International Symposium on Friction Stir Welding, Sweden.
- [10] Schmidt, H. N. B., Hattel, J. H., and Wert, J., "An Analytical Model for the Heat Generation in Friction Stir Welding," *Modeling and Simulation in Materials Science and Engineering*, 12(1), 143–157, 2004.
- [11] Tartakovsky, A., Grant, G., Sun, X., and Khaleel, M., "Modeling of Friction Stir Welding (FSW) Process with Smooth Particle Hydrodynamics (SPH)," *SAE Technical Paper 2006-01-1394*, 2006, doi:10.4271/2006-01-1394.
- [12] I. Alfaro, G. Racineux, A. Poitou, E. Cueto, and F. Chinesta, "Numerical Simulation of Friction Stir Welding " *International Journal of Material Forming* 2, 225–234, 2009.
- [13] DYNA3D, Livermore Software Technology Corporation, <http://www.lstc.com> [cited 2016].
- [14] Benz, W., "Smooth particle hydrodynamics: A review," in *The Numerical Modelling of Nonlinear Stellar Pulsations*, ed. J. R. Buchler, editor, 269–288, Kluwer Academic Publishers, 1990.
- [15] Lacombe, J. L. "SPH—Part I and II," Livermore Software Technology Corporation, 2001.
- [16] Livermore Software Technology Corporation, *LS-DYNA Keyword Manual*, version 971, 1998, <http://www.lstc.com> [cited 2012].
- [17] Ulysse, Patrick, 2002, "Three-dimensional Modeling of the Friction Stir Welding Process", *International Journal of Machine Tools & Manufacture*, p 1549-1557.
- [18] Feng, Z., Santella, M. L., David, S. A., Steel, R. J., Packer, S. M., Pan, T., Kuo, M., and Bhatnagar, R.S., "Friction stir spot welding of advanced high-strength steels –A feasibility study, *SAE Technical Paper 2005-01-1248*, 2005, doi:10.4271/2005-01-1248.
- [19] Johnson, G. R., and Cook, W. H., "A constitutive model and data for metal subjected to large strain, high strain rate and high temperature," *Proceedings of 7th International Symposium on Ballistics*, The Hague, The Netherlands, April 1983, pp. 541–548.
- [20] Khandkar, M.Z.H., "Thermo-mechanical modeling of friction stir welding," Ph.D. Dissertation, University of South Carolina, 2005.
- [21] Xu, L., and Khan, J. A., "Nugget growth model for aluminum alloys during resistance spot welding," *Welding Journal*, 78(11), 367–372, 1999
- [22] Hallquist, J. O., *LS-DYNA Theory Manual*, Livermore Software Technology Corporation, 2006.
- [23] Gerlich, A., Su, P., North, T. H., "Tool penetration during friction stir spot welding of Al and Mg alloys," *Journal of Materials Science*, 40(24), 6473–6481, Dec 2005.
- [24] http://www.hzg.de/institute/materials_research/structure/materials_mechanics/solid_state_joining_processes/publications/index.html.de, Helmholtz-Zentrum Geeshacht, [cited 2016].
- [25] Bhojwani, S., "Smoothed particle hydrodynamics modeling of the friction stir welding process," M.S. Thesis, University of Texas at El Paso, January 2007.